
Equivalence analysis between Quasi-coarse-grained and Atomistic Simulations

Dong-Dong Jiang¹, Jian-Li Shao^{1,2*}

¹ National Key Laboratory of Explosive Science and Safety Protection, Beijing Institute of Technology, Beijing, 100081, China

² Explosion Protection and Emergency Disposal Technology Engineering Research Center of the Ministry of Education, Beijing, 100039, China

Abstract

In recent years, simulation methods based on the scaling of atomic potential functions, such as quasi-coarse-grained dynamics and coarse-grained dynamics, have shown promising results for modeling crystalline systems at multiple scales. However, this letter presents evidence suggesting that the spatiotemporal trajectories of coarse-grained systems generated by such simulation methods exhibit a complete correspondence with those of specific molecular dynamics systems. In essence, current coarse-grained simulation methods involve a direct amplification of the results obtained from molecular dynamics simulations across spatial and temporal scales, yet they may lack the capability to adequately capture authentic scale effects. Consequently, the findings of related studies warrant careful re-evaluation. Furthermore, this study underscores the importance of not only verifying the consistency of mesoscale simulation methods with microscopic simulations but also meticulously assessing their capability to accurately forecast mesoscale physical phenomena.

Keywords: Mesoscale Modelling; Coarse-grained Dynamics; Molecular Dynamics.

*Corresponding author, email: shao_jianli@bit.edu.cn

The importance of molecular dynamics (MD) simulations in advancing materials science and engineering cannot be overstated. These simulations offer a window into the fundamental nature of the world at the atomic scale, disregarding quantum effects. However, MD simulations have long grappled with two significant challenges. Firstly, their simulation outcomes hinge entirely upon the interatomic potential function, which has historically been scrutinized due to its reliance on model approximations and empirical parameters [1]. Secondly, MD simulations demand substantial computational resources, with the number of particles in macroscopic entities surpassing the computational capabilities of current supercomputers. The spatial and temporal scale of the largest all-atom MD simulations recorded to date are limited to the micrometer and microsecond [2], with the majority confined to the nanometer and nanosecond scales. This limitation makes it challenging to directly apply MD simulations to macroscopic dynamic problems across different length scales and to assess size effects between microscopic physical processes and macroscopic phenomena. In recent years, significant strides have been made in addressing the first challenge through the development of machine learning potential functions based on first principles. These advancements have enabled MD simulations with first-principles accuracy on scales exceeding a hundred million atoms, thereby significantly enhancing their reliability [3,4]. On the other hand, numerous mesoscopic simulation methods have emerged. Examples include coarse-grained MD for materials systems characterized by clear structural hierarchies, such as proteins and polymers [5–7], and dissipative particle dynamics for complex fluid systems [8,9]. These methods have been widely and successfully applied. However, for typical crystalline materials like metals and ceramics, the macroscopic mechanical behavior correlates with various microscopic-scale structural evolutions, such as dislocations and twinning [2,10,11]. In these microstructural evolution processes, interactions between individual atoms exert equally significant influences, distinguishing them from the selective bundling of particles in large molecular systems. Consequently, direct application of traditional coarse-graining methods to crystalline systems poses challenges.

Currently, mesoscopic simulation methods for crystalline systems can generally be categorized into two main types: mesoscopic theoretical simulation methods and concurrent multiscale coupling simulation methods. The former abstractly model actual material deformation and phase transition processes based on physical understanding, examples include phase-field dynamics [12–15] and discrete dislocation dynamics [16,17]. These methods heavily rely on empirical knowledge of physical laws and face challenges in handling various types of defects and interactions among different structures in practical processes. The latter category involves the use of full-atom molecular dynamics simulations to predict localized deformation and damage, coupled with macroscopic simulation methods like finite element analysis in other regions [18–20]. The exchange of physical information such as momentum and heat between the two regions enables their direct coupling, which has shown promising applications in problems like crack propagation [21,22]. However, when deformation and damage within the material are relatively uniform, such methods encounter significant difficulties. This is because the macroscopic simulation region struggles to accurately capture the thermodynamic effects of various physical processes like structural damage and phase transition. Particularly, numerous studies have indicated strong size effects and strain rate effects in processes such as damage [23,24], phase transition [25], and plastic deformation of crystalline materials [11,26], necessitating direct mesoscopic scale investigations into these processes.

To address the challenges encountered in simulating the mesoscale behavior of crystal materials, Dongare et al. [27] proposed a quasi-coarse-grained dynamic simulation method. This approach relies on representative particles to capture the overall dynamic behavior, leveraging the symmetry and periodicity inherent in crystal structures. By directly scaling the atomic potentials, the interactions between these representative particles are effectively modeled. This methodology offers the flexibility to scale the spatiotemporal scales of MD simulations by arbitrary factors, while still preserving crucial microscopic structural evolution details. It is considered a promising development route for multiscale simulations and has been applied to explore various mesoscale physical phenomena such as particle cold spraying [28], phase transitions [29], void collapse [30], and shock wave front evolution [31]. It has also found some applications in graphene and silicon [32]. Although the fundamental concept of this method originates from the structural characteristics of crystals, it is equally applicable to molten liquid systems. It has been successfully applied to the micro-spallation behavior in molten metals [33]. Furthermore, based on similar ideas to quasi-coarse-grained dynamics, there have emerged methods that directly aggregate the energy and mass of atoms within specific regions into single particles for coarse-grained simulations of crystals [34,35].

In summary, research on quasi-coarse-grained simulations of crystal materials represents a crucial direction in micro-meso-scale simulation. However, we will demonstrate here simply and reliably that the above quasi-coarse-grained dynamics, as well as coarse-grained simulation, are completely equivalent to full atomic-scale molecular dynamics simulations at the microscale. Therefore, quasi-coarse-grained simulations at any scale are equivalent to MD simulations.

To begin, let's review the basic principles of MD and quasi-coarse-grained dynamics. In the realm of MD simulation methods, a crucial step involves determining the potential energy E_i associated with each atom based on its atomic configuration. This process allows for the derivation of the corresponding forces F_i acting on these atoms, as delineated by Equations (1) and (2). Notably, the function Φ within these equations can assume various forms, encompassing potential functions such as pair potentials, many-body potentials, and even machine learning potentials.

$$E_i^{atom} = \Phi(\mathbf{r}_i) \quad (1)$$

In which \mathbf{r}_i denotes the set of relative positions between the i atom and all other atoms with which it interacts.

$$\mathbf{F}_i^{atom} = -\frac{\partial E_i^{atom}}{\partial \mathbf{R}_i} \quad (2)$$

\mathbf{R}_i refers to the coordinate vector of atom i . After obtaining the force acting on the atom, the position of atom i at the next moment can be obtained based on Newtonian mechanics theory and initial information on the atomic position and velocity, gradually obtaining the spatiotemporal trajectories of all atoms.

In quasi-coarse-grained dynamics [27], representative atoms are proposed to characterize the average properties of all atoms within a specific region. These representative atoms possess identical neighborhood structural features as the initial atomic system. As depicted in Fig. 1, the all-atomic (AA) system with FCC structure in Fig. 1(a) can be represented by the quasi-coarse-grained (QCG) system composed of representative particles (R-particles) shown

in Fig. 1(b). The QCG system has the same structure and orientation as the AA system, but with a larger lattice constant. The factor by which the lattice constant increases is termed the distance scaling parameter (A_{cg}). The terminology $L_{A_{cg}}$ is used to represent the coarsening level adopted in the method. Consequently, each R particle represents the average properties of A_{cg}^3 atoms. In the example depicted in Fig. 1, $A_{cg}=2$. Importantly, this parameter need not be an integer; it merely requires the final QCG system to exhibit consistent shape and volume with the full atomic system.

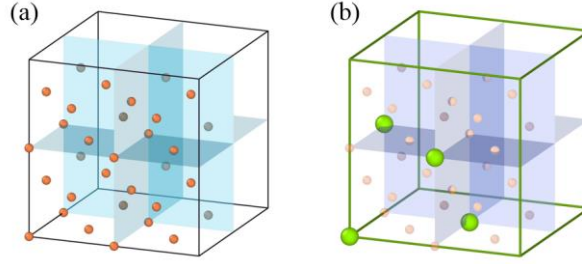


Fig. 1 All-atomic system **(a)** and corresponding quasi-coarse-grained system **(b)**

After constructing the QCG system, another key aspect of QCGD simulations lies in defining the interaction potential between R-particles. Given the similarity in neighborhood structure between the QCG and AA systems, the potential function between R particles can be derived by directly scaling the interatomic potential function, as shown in Equation (3):

$$E_i^R = \Phi\left(\frac{\mathbf{r}_i}{A_{cg}}\right) \quad (3)$$

Based on this potential function, R-particles at any strain can maintain the same energy characteristics as atoms in MD simulations. After introducing the total energy, stress, and temperature calculation methods related to the parameter A_{cg} [27], the QCG system can predict thermodynamic properties such as temperature and pressure that are almost identical to those of the AA system. In addition, due to the complete preservation of the shape of the original interatomic potential function by the QCG potential function, it is completely consistent with MD simulations on various structural potential barriers, such as stacking fault energy and phase to phase nuclear energy. At the same time, in order to ensure the consistency of particle mass related dynamic characteristics such as wave velocity, thermal conductivity, and MD simulations, it is necessary to have the mass of the representative particle R equal to the atomic mass, which is also consistent with the definition of the representative particle. The above QCGD simulation has been verified to be consistent with MD simulation in many properties such as melting point, melting rate, shock wave velocity, dislocation velocity, etc.

However, a new issue is that the capability of QCGD to describe scale effects as the distance scaling parameter increases remains unproven. Here we consider an arbitrary quasi-coarse-grained system, where the set of coordinates of all R atoms at time t is denoted as \mathbf{R}_t^R . There exists a corresponding all-atom system, a direct scaled down of the CG system in space, where the set of coordinates of all atoms is denoted as $\mathbf{R}_t^{\text{atom}}$, i.e.

$$\mathbf{R}_t^{atom} = \frac{\mathbf{R}_t^R}{A_{cg}} \quad (4)$$

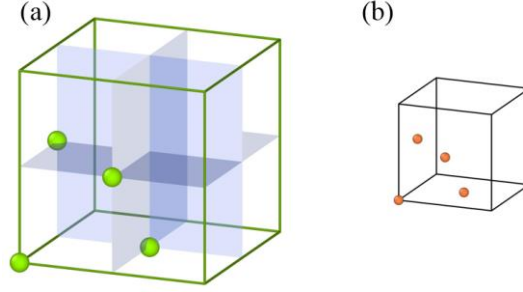


Fig. 2 Quasi-coarse-grained system and corresponding scaled down all-atom system

Since the QCG system is constructed with the same structural arrangement as the AA system (as shown in Figure 1), the corresponding reduced atomic configuration \mathbf{R}_t^{atom} also represents a real physical system. Additionally, we set the atom velocities of this atomic system to:

$$\mathbf{v}_t^{atom} = \mathbf{v}_t^R \quad (5)$$

At this velocity setting, the average kinetic energy of atoms in the atomic system is consistent with the average kinetic energy of particles in the QCG system, indicating that the initial temperatures of the two systems are exactly the same.

Under the above initial conditions, consider the independent subsequent evolution of these two systems. Combining equations (1)-(4), it can be concluded that for any R-particle i and its corresponding atom i , there are:

$$\mathbf{F}_i^R = \frac{\mathbf{F}_i^{atom}}{A_{cg}} \quad (6)$$

Combining $m^R = m^{atom}$, there is $\mathbf{a}^R = \frac{\mathbf{a}^{atom}}{A_{cg}}$. After Δt time, the set of coordinates of all atoms is:

$$\mathbf{R}_{t+\Delta t}^{atom} = \mathbf{R}_t^{atom} + \mathbf{v}_t^{atom} \Delta t + \frac{1}{2} \mathbf{a}^{atom} \Delta t^2 \quad (7)$$

Correspondingly, after $A_{cg} \Delta t$ time, the quasi coarse-grained system has:

$$\mathbf{R}_{t+A_{cg}\Delta t}^R = \mathbf{R}_t^R + A_{cg} \mathbf{v}_t^R \Delta t + \frac{1}{2} \mathbf{a}^R A_{cg}^2 \Delta t^2 \quad (8)$$

Substituting equations (4) and (5) yields:

$$\mathbf{R}_{t+A_{cg}\Delta t}^R = A_{cg} \mathbf{R}_{t+\Delta t}^{atom} \quad (9)$$

At the same time, it is easy to obtain:

$$\mathbf{v}_{t+A_{cg}\Delta t}^R = \mathbf{v}_{t+\Delta t}^{atom} \quad (10)$$

This implies that for any QCG system, there exists a corresponding AA system, and the two systems show complete correspondence in their subsequent spatiotemporal evolution. Hence, it stands to reason that a QCGD simulation can reproduce all physical properties and evolutionary behaviors observed in molecular dynamics simulations under identical stress and temperature conditions. Nevertheless, this also rules out the possibility of utilizing increase coarsening level to capture any mesoscale behavior.

In practical simulations, the time step of the QCG system can be set to A_{cg} times that of the MD simulation system. By combining this with Equation 9, it is theoretically observed that the particle positions and velocities of the QCG system align perfectly with those of the AA system after the same number of steps. It is important to ensure that the corrections to particle positions and velocities are consistently applied at each step. Under this condition, artificial loading such as impacts, tensile/compressive deformations, and ensemble corrections will not disrupt this alignment. Taking the example of uniaxial compression of single crystal copper with constant volume, the time step for the AA system is 2 fs, and the strain rate is 1×10^{10} /s. When A_{cg} is 10, the time step becomes 20 fs, corresponding to a compression strain rate of 1×10^9 /s. When A_{cg} increase to 100, the strain rate further reduces to 1×10^8 /s. This setting ensures that the three models are compressed by the same proportion at each time step. The specific simulation results are depicted in Figure 3. In the initial thousands of steps, the three simulations exhibit complete correspondence, with stress-strain curves perfectly overlapping. Even the positions, velocities, and local structures of each atom are identical (as shown in the left images of Figure 3b and c), consistent with our previous demonstration. However, as the simulation progresses, at strain values greater than 0.1, the stress-strain curves of the three models no longer overlap completely. Nevertheless, they still follow consistent evolution patterns. From the comparison of particle neighborhood structures in the right images of Figure 3b and c, it can be observed that the particle structure characteristics of the AA system and the L100 QCG system remain consistent, albeit specific dislocation and stacking fault positions show some differences. This discrepancy arises from floating-point math not being associative and the chaotic nature of MD simulations. During the QCGD simulation process, scaling the potential function and system coordinates can introduce minimal numerical errors, causing slight differences and eventual divergence of molecular dynamics phase space trajectories within a few thousand timesteps. However, the statistical properties of the two runs (e.g., average energy or temperature) should remain consistent. Therefore, these minor differences resulting from the chaotic nature of the system do not affect the correspondence between the two systems as demonstrated above. In summary, the simulations above demonstrate that although the strain rates of these three systems differ by a factor of 100, the stress-strain curves are nearly identical, fully proving the consistency between all-atom simulations and QCGD simulations after temporal and spatial scaling.

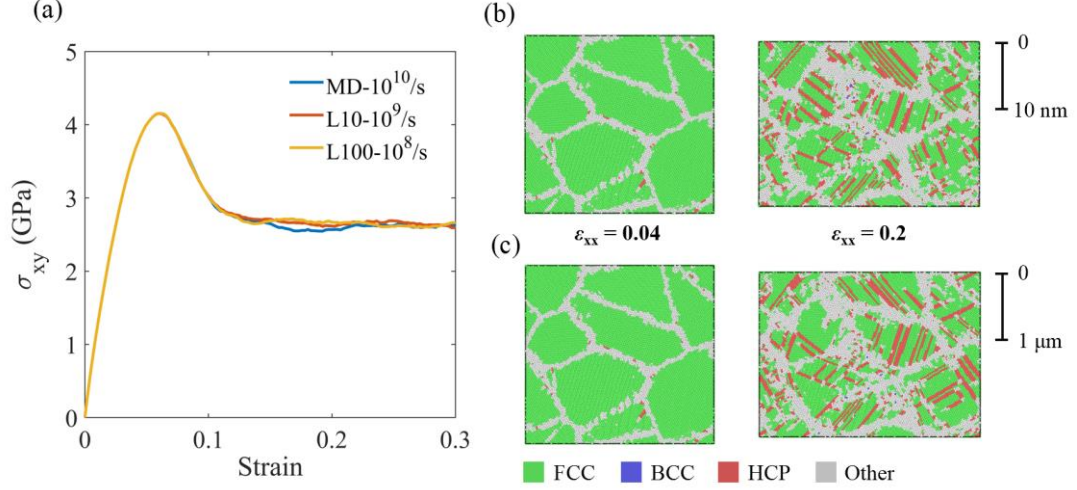


Fig. 3 (a) Evolution of shear stress during compression process; (b) Atomic local configurations obtained from molecular dynamics simulations at different strains; (c) Particle local configurations obtained from coarse-grained dynamics simulations at different strains.

In CGMD simulations, unlike QCGD simulations, each coarse-grained particle no longer represents the average property of atoms within a specific region, but directly replaces all atoms in the region. Therefore, its particle mass is the sum of atomic masses within the region, i.e., $m^{CG} = A_{cg}^3 m^{atom}$. The relationship between the potential energy of coarse-grained particles and the potential energy of atoms is:

$$E_i^R = A_{cg}^3 \Phi\left(\frac{\mathbf{r}_i}{A_{cg}}\right) \quad (11)$$

The CGMD simulation method, in contrast to the QCGD approach, naturally preserves the same mass density and total energy density as the atomic system without necessitating additional conversions. However, akin to QCGD, for any coarse-grained system, there exists a corresponding all-atom system, conforming to the relationships articulated in Equation 4 and Equation 5. Specifically, for any i particle and its corresponding i atom, $\mathbf{r}_i^{CG} = A_{cg} \mathbf{r}_i^{atom}$. Combining Equations 1, 2, and 11, we obtain $\mathbf{F}_i^R = A_{cg}^2 \mathbf{F}_i^{atom}$. Taking into account the correspondence between the mass of coarse-grained particles and that of atoms, similar to QCMD, we still find $\mathbf{a}^R = \frac{\mathbf{a}^{atom}}{A_{cg}}$. Thus, akin to QCGD, subsequent particle trajectories in CGMD simulations align precisely with the

atomic trajectories of the all-atom system. The related thermodynamic properties and microscopic physical attributes are also entirely consistent. Evidently, CGMD lacks fundamental disparity from QCGD.

Below, we illustrate how the QCGD and CGMD simulation methods have demonstrated misleading scale effects, using the example of the shock loading process of polycrystalline aluminum. For instance, when investigating the impact of grain size on shock wave profiles, we vary the coarsening level to generate models of varying grain sizes. The configurations of all simulation groups are outlined in Table 1, and the resulting simulations are depicted in Fig. 4. Initially, MD simulations and QCGD simulations with different coarsening level were employed to calculate the

shock loading process of the same model. Fig. 4(a) and (b) show the characteristics of shock waveforms and the attenuation of precursor amplitudes with increasing shock depth. It can be observed that the results of QCGD simulations are not significantly different from those of MD simulations. This similarity is often used to demonstrate that quasi-coarse-grained methods are reliable approximations of MD simulations.

Table 1. Initial model setup for polycrystalline aluminum shock simulation.

Num	Coarsening Level	Particle Count	Model size (nm³)	Grain Sizes (nm)
1	L1	86259771	60×60×400	25.5
2	L2	10770843	60×60×400	25.5
3	L4	1345193	60×60×400	25.5
4	L1	10770843	30×30×200	12.8
5	L2	10770843	60×60×400	25.5
6	L4	10770843	120×120×800	51.0
7	L8	10770843	240×240×1600	102
8	L16	10770843	480×480×3200	204

Furthermore, by adjusting the coarsening level, models with the same number of particles can be used to study the influence of grain size on the attenuation behavior of elastic precursor waves. As shown in Fig. 4(c), the results indicate that larger grain sizes lead to slower attenuation of elastic precursor waves. However, as demonstrated earlier in this paper, the simulation results of different grain sizes are actually just different manifestations of simulations of the same all-atomic model, rather than differences in the physical properties of systems brought about by different grain sizes. If the shock depth on the abscissa in Fig. 4(c) is changed to the proportion of the shock depth to the entire model, as shown in Fig. 4(d), it can be observed that these groups of simulations exhibit completely consistent patterns, with only minor differences due to random thermal fluctuations in the system.

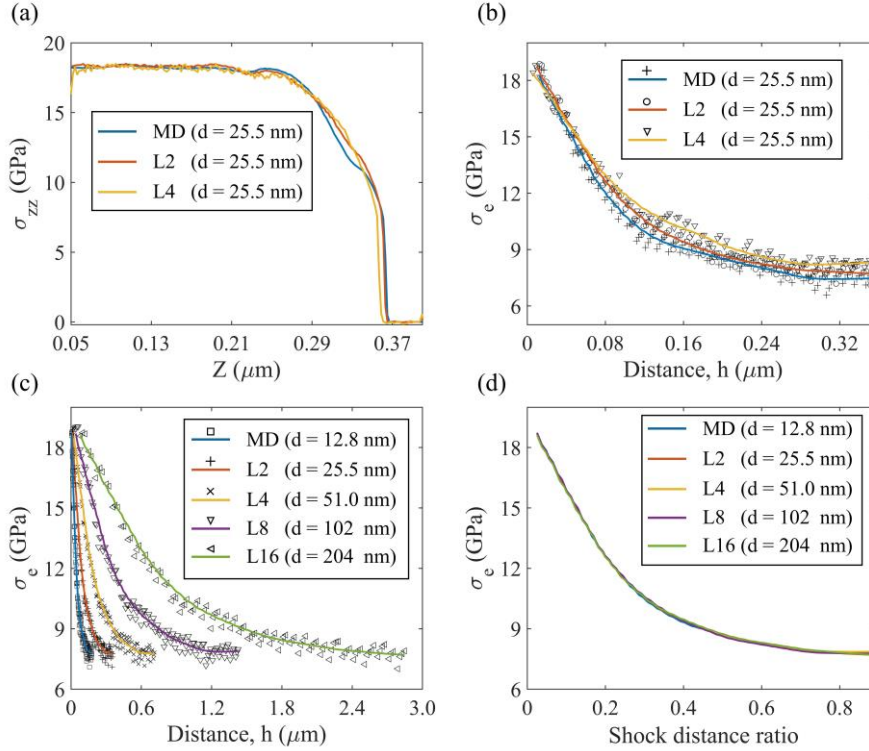


Fig. 4 (a) Shock wave profiles under different coarsening level; (b) Attenuation of elastic precursor amplitude with shock depth under varying coarsening level; (c) Attenuation of elastic precursor amplitude with shock depth under different grain sizes; (d) Attenuation of elastic precursor amplitude with shock ratio (ratio of shock depth to sample thickness) under different grain sizes.

The above results further confirm the complete correspondence between the QCGD simulations results and the corresponding all-atom simulation results. However, due to the direct amplification of MD simulation results in both time and space dimensions, certain physical phenomena may exhibit false size-effect characteristics, potentially leading researchers to overlook this crucial issue. Recognizing that the reduction of system degrees of freedom during coarse-graining inevitably leads to the loss of physical information, a potential solution lies in compensating for this loss by incorporating intrinsic physical quantities onto coarse-grained particles. This could prove pivotal in ensuring the effectiveness of mesoscopic simulations.

Indeed, virtually all multiscale simulation approaches stemming from microscopic simulations encounter this challenge [37–39]. In addition to verifying the consistency between mesoscopic simulation results and their full atomic counterparts, it is imperative to meticulously evaluate their capacity to accurately capture mesoscale physical phenomena.

Funding: This work is supported by the National Key R&D Program of China (Grant No. 2021YFB3802300).

References

- [1] Y. Mishin, M. Asta, J. Li, Atomistic modeling of interfaces and their impact on microstructure and properties, *Acta Mater.* 58 (2010) 1117–1151.
- [2] L.A. Zepeda-Ruiz, A. Stukowski, T. Opperstrup, V. V. Bulatov, Probing the limits of metal plasticity with

molecular dynamics simulations, *Nature* 550 (2017) 492–495.

[3] B. Dou, Z. Zhu, E. Merkurjev, L. Ke, L. Chen, J. Jiang, Y. Zhu, J. Liu, B. Zhang, G.W. Wei, *Machine Learning Methods for Small Data Challenges in Molecular Science*, *Chem. Rev.* 123 (2023) 8736–8780.

[4] T. Wen, L. Zhang, H. Wang, W. E, D.J. Srolovitz, *Deep potentials for materials science*, *Mater. Futur.* 1 (2022) 022601.

[5] B.A. Merchant, J.D. Madura, *A Review of Coarse-Grained Molecular Dynamics Techniques to Access Extended Spatial and Temporal Scales in Biomolecular Simulations*, in: 2011: pp. 67–87.

[6] S.Y. Joshi, S.A. Deshmukh, *A review of advancements in coarse-grained molecular dynamics simulations*, *Mol. Simul.* 47 (2021) 786–803.

[7] J. Wang, S. Olsson, C. Wehmeyer, A. Pérez, N.E. Charron, G. de Fabritiis, F. Noé, C. Clementi, *Machine Learning of Coarse-Grained Molecular Dynamics Force Fields*, *ACS Cent. Sci.* 5 (2019) 755–767.

[8] P. Español, P. Warren, *Statistical Mechanics of Dissipative Particle Dynamics*, *Europhys. Lett.* 30 (1995) 191–196.

[9] P. Español, P.B. Warren, *Perspective: Dissipative particle dynamics*, *J. Chem. Phys.* 146 (2017).

[10] T.P. Remington, E.N. Hahn, S. Zhao, R. Flanagan, J.C.E. Mertens, S. Sabbaghianrad, T.G. Langdon, C.E. Wehrenberg, B.R. Maddox, D.C. Swift, B.A. Remington, N. Chawla, M.A. Meyers, *Spall strength dependence on grain size and strain rate in tantalum*, *Acta Mater.* 158 (2018) 313–329.

[11] W. Li, E.N. Hahn, X. Yao, T.C. Germann, X. Zhang, *Shock induced damage and fracture in SiC at elevated temperature and high strain rate*, *Acta Mater.* 167 (2019) 51–70.

[12] D. Simeone, *Dynamics of Nucleation in Solids : A Self-Consistent Phase Field Approach*, *Phys. Rev. Lett.* 131 (2023) 117101.

[13] Rahul, S. De, *A phase-field model for shock-induced α - γ Phase transition of RDX*, *Int. J. Plast.* 88 (2017) 140–158.

[14] A. Karma, D.A. Kessler, H. Levine, *Phase-Field Model of Mode III Dynamic Fracture*, *Phys. Rev. Lett.* 87 (2001) 045501.

[15] Z. Li, T. Wang, D. Chu, Z. Liu, Y. Cui, *A coupled crystal-plasticity and phase-field model for understanding fracture behaviors of single crystal tungsten*, *Int. J. Plast.* 157 (2022) 103375.

[16] E. Van der Giessen, A. Needleman, *Discrete dislocation plasticity: a simple planar model*, *Model. Simul. Mater. Sci. Eng.* 3 (1995) 689–735.

[17] L.E. Shilkrot, R.E. Miller, W.A. Curtin, *Coupled Atomistic and Discrete Dislocation Plasticity*, *Phys. Rev. Lett.* 89 (2002) 025501.

[18] P. Wurm, M.H. Ulz, *Demand-based coupling of the scales in concurrent atomistic-to-continuum models at finite temperature*, *J. Mech. Phys. Solids* 137 (2020).

[19] S. Kohlhoff, P. Gumbsch, H.F. Fischmeister, *Crack propagation in b.c.c. crystals studied with a combined finite-element and atomistic model*, *Philos. Mag. A* 64 (1991) 851–878.

[20] J.Q. Broughton, F.F. Abraham, N. Bernstein, E. Kaxiras, *Concurrent coupling of length scales: Methodology and application*, *Phys. Rev. B* 60 (1999) 2391–2403.

[21] C.L. Rountree, R.K. Kalia, E. Lidorikis, A. Nakano, L. Van Brutzel, P. Vashishta, *Atomistic Aspects of Crack Propagation in Brittle Materials: Multimillion Atom Molecular Dynamics Simulations*, *Annu. Rev. Mater. Res.* 32 (2002) 377–400.

[22] Z. Wang, Q. Dong, N. Guo, M.R. Daymond, *Crack propagation path selection and plastic deformation at a crack tip in zirconium*, *Mater. Sci. Eng. A* 779 (2020) 139143.

-
- [23] Y. Cai, J.Y. Huang, H.A. Wu, M.H. Zhu, W.A. Goddard, S.N. Luo, Tensile Strength of Liquids: Equivalence of Temporal and Spatial Scales in Cavitation, *J. Phys. Chem. Lett.* 7 (2016) 806–810.
- [24] J.W. Wilkerson, K.T. Ramesh, Unraveling the anomalous grain size dependence of cavitation, *Phys. Rev. Lett.* 117 (2016) 1–5.
- [25] P.A. Santos-Florez, H. Yanxon, B. Kang, Y. Yao, Q. Zhu, Size-Dependent Nucleation in Crystal Phase Transition from Machine Learning Metadynamics, *Phys. Rev. Lett.* 129 (2022) 185701.
- [26] Q. Yu, Z.-W. Shan, J. Li, X. Huang, L. Xiao, J. Sun, E. Ma, Strong crystal size effect on deformation twinning, *Nature* 463 (2010) 335–338.
- [27] A.M. Dongare, Quasi-coarse-grained dynamics: Modelling of metallic materials at mesoscales, *Philos. Mag.* 94 (2014) 3877–3897.
- [28] S. Suresh, S.-W.W. Lee, M. Aindow, H.D. Brody, V.K. Champagne, A.M. Dongare, Mesoscale modeling of jet initiation behavior and microstructural evolution during cold spray single particle impact, *Acta Mater.* 182 (2020) 197–206.
- [29] A.M. Dongare, Challenges to model the role of heterogeneities on the shock response and spall failure of metallic materials at the mesoscales, *J. Mater. Sci.* 55 (2020) 3157–3166.
- [30] S. Galitskiy, A. Mishra, A.M. Dongare, Modeling shock-induced void collapse in single-crystal Ta systems at the mesoscales, *Int. J. Plast.* 164 (2023).
- [31] G. Agarwal, R.R. Valisetty, A.M. Dongare, Shock wave compression behavior and dislocation density evolution in Al microstructures at the atomic scales and the mesoscales, *Int. J. Plast.* 128 (2020) 102678.
- [32] K. Mohammadi, A. Ali Madadi, Z. Bajalan, H. Nejat Pishkenari, A.A. Madadi, Z. Bajalan, H.N. Pishkenari, Analysis of mechanical and thermal properties of carbon and silicon nanomaterials using a coarse-grained molecular dynamics method, *Int. J. Mech. Sci.* 187 (2020) 106112.
- [33] P. Chen, X. Wang, P. Wang, A.-M. He, A mesoscale study of micro-spallation of Cu through coarse-grained molecular dynamics modeling, *Int. J. Mech. Sci.* 220 (2022).
- [34] A.A. Madadi, A.R. Khoei, A coarse-grained-Atomistic multi-scale method to study the mechanical behavior of heterogeneous FCC nano-materials, *Comput. Mater. Sci.* 199 (2021).
- [35] L. Chalamet, D. Rodney, Y. Shibuta, Coarse-grained molecular dynamic model for metallic materials, *Comput. Mater. Sci.* 228 (2023) 112306.
- [36] G. Agarwal, A.M. Dongare, Defect and damage evolution during spallation of single crystal Al: Comparison between molecular dynamics and quasi-coarse-grained dynamics simulations, *Comput. Mater. Sci.* 145 (2018) 68–79.
- [37] B. Goh, J. Choi, A spatial upscaling method for describing the three-body potential of a diamond lattice structure, *Appl. Math. Model.* 108 (2022) 502–511.
- [38] M. Jahanshahi, M. Vokhshoori, A.R. Khoei, A coarse-graining approach for modeling nonlinear mechanical behavior of FCC nano-crystals, *Comput. Mater. Sci.* 172 (2020) 109357.
- [39] B. Goh, J. Choi, Subcontinuum scale analysis of diamond lattice films through spatial multi-level coarsening method, *Thin-Walled Struct.* 187 (2023) 110738.